Journal of the Iowa Academy of Science: JIAS

Volume 100 | Number Article 3

1993

Advances in Biomolecule Analysis: FTMS of Macromolecules

Curtiss D. Hanson
University of Northern Iowa

Ira M. Simet
University of Northern Iowa

Suzanne R. Smith
University of Northern Iowa

Jour. Iowa Acad. Sci. 100(1):1-8, 1993

Advances in Biomolecule Analysis: FTMS of Macromolecules

CURTISS D. HANSON, IRA M. SIMET, and SUZANNE R. SMITH

University of Northern Iowa, Department of Chemistry, Cedar Falls, IA 50614-0423

The development of Fourier transform ion cyclotron resonance (*FT-ICR*) as an analytical technique has opened new avenues to the analysis of high molecular weight biomolecules. Because mass analysis is based on a detection of a frequency, it is possible to obtain high resolution mass measurements without sacrificing sensitivity. The unique ability to analyze high mass ions is based in the design of a passive ExB ion trap. Although in the past, field inhomogeneities have limited this technique, recent developments in both trap designs and excitation techniques have resulted in major improvements in both sensitivity and resolution.

INDEX DESCRIPTORS: Fourier transform ion cyclotron resonance, mass spectrometry of biomolecules, ion trap design, high mass analysis.

Biomolecules have always presented chemists with the problem of analyzing fairly complex molecules which occur in only trace quantities. Prior to the availability of mass spectrometry, a pure compound had to be isolated from mixtures of natural products using repeated extractions and recrystallization. The molecular weights of the sample molecule or its degradation products could be estimated using cryoscopic or osmotic techniques that provided limited resolution (*1*). The application of mass spectrometry to biomolecule analysis provided a rapid technique that could provide high resolution mass measurements with extreme sensitivity.

Although magnetic-deflection or sector-type mass spectrometers are capable of high resolution mass measurements, such precision can only be obtained at the expense of sensitivity. Following the adaptation of suitable ionization methods for large, involatile, thermally labile biomolecules, a large thrust in the research surrounding Fourier transform ion cyclotron resonance (*FT-ICR*) development has emphasized detection at high mass and high resolution at high mass (*2*). The high resolution, coupled with technical advancements in ionization methods (*3,4,5,*) and a vacuum interlock for sample introduction (*6*), has resulted in the evolution of high performance FT-ICR instruments.

While the applicability of FT-ICR to characterization of high molecular weight biomolecules has long been appreciated, realization of its potential depended on improvements in desorption methodology. The large size and inherent lability of biomolecules prevented their volatilization and ionization by techniques developed for small-mass molecules. These obstacles persisted until the 1980's, but they have been largely overcome through the modernization of older approaches and the introduction of newer techniques.

Initial successes with biomolecules were attained with fast atom bombardment (*FAB*) of insulin (*7*) and other small proteins. Subsequently, desorption and ionization were achieved by bombardment of nonvolatile biomolecules, dissolved in volatile glycerol matrices, with fast ions, chiefly Cs^+ (*8,9*). This technique, liquid-secondary ion mass spectrometry (*L-SIMS*), also featured utilization of a tandem spectrometer in which ions produced in a differentially pumped quadrupole source were transferred to an FT-ICR analyzer. Use of L-SIMS expanded the range of observable molecular weights to approximately 13,000, as shown by the analysis of horse cytochrome c (*molecular weight 12,384*) (*10*).

Plasma desorption (*PD*), another collision-based method that uses ions produced by fission of ^{252}Cf, was demonstrated to be suitable for resolution and analysis of a variety of proteins, including porcine trypsin (*molecular weight 23,460*) (*11,12*) and chicken ovalbumin (*molecular weight 45,000*) (*12*). It also was valuable in mass spectrometric determinations of base sequences of oligoribonucleotides containing non-hydrolyzable, non-phosphodiester linkages (*13,14*). This technique was combined with FT-ICR in characterization of peptides and small proteins such as leu-enkephalin (*15*) and gramicidin S (*16*).

Alternatives to particle bombardments have also been described for biomolecules. Laser desorption (*LD*), first shown to be applicable for analysis of biomolecules in 1978 (*17*), uses photons to volatilize and ionize target molecules. This technique has recently increased the threshold size for analysis of large molecules by nearly an order of magnitude. For example, jack bean urease, a polypeptide larger than 250,000 daltons, has been ionized and analyzed by time of flight mass spectrometry (*TOFMS*) (*18*). Application of LD to FT-ICR has proved efficient for analysis of proteins, polysaccharides, and several other classes of biomolecules.

Two additional advantages accrue with biomolecule ion generation by PD and LD. Each of these techniques can produce multiply-charged ions, which increases the theoretical maximal mass limit for instruments of fixed *m/q* capability. This phenomenon is particularly notable for plasma desorption of biomolecules adsorbed on nitrocellulose films (*19*). Mathematical transformations can establish the charge density of measured peaks while helping to identify background signals (*20*). Also, these techniques induce less fragmentation of large ions, which greatly simplifies the mass spectra obtained by FT-ICR. The enhanced lifetime of the original high mass ions, coupled with their resistance to collisional scattering, allows them to be re-excited to larger orbits for remeasurement; the resulting increase in sensitivity of detection therefore can offset the low efficiency of desorption of these large biomolecules (*21*).

The advantage of multiply-charged ions has been taken one step further by the recent emergence of electrospray ionization (*ESI*) as a desorptive method. Suggestions that this technique would be ideal for large biomolecules were made as early as 1968 (*22*). Using ESI, highly charged droplets of a solution containing a biomolecule are produced electrically. As these droplets move through an electrical field with a counterflow of dry gas, the solvent is lost progressively. The resulting species, large molecular ions of multiple charge with some associated neutral solvent molecules, can then be analyzed by FT-ICR. The multiple charging affords an upper *m/q* of approximately 1500 for a variety of proteins (*23,24*), with success up to a total mass of nearly 133,000 (*25*).

The application of these desorptive techniques to FT-ICR makes mass spectrometry an attractive alternative to many analytical procedures currently in use in biochemistry. For example, biochemical determinations of peptide and protein molecular weights suffer from limitations in applicability, sensitivity, and precision. Sodium dodecyl sulfate-polyacrylamide gel electrophoresis (*SDS-PAGE*), the predominant method used for size assessment since its introduction by Laemmli in 1967 (*26*), can be used for a majority of proteins. However, anomalies in SDS binding generally compromise the use of this technique for analysis of glycoproteins and highly acidic proteins. Gel filtration chromatography, an alternative technique, also fails in these cases due to the irregular shapes and aggregative behaviors of the

molecules. The use of FT-ICR overcomes these difficulties by obviating the need for chaotropes and by elimination of the dependence on shape factors.

Even for those molecules well-suited for SDS-PAGE analysis, post-separation detection can limit sensitivity. Traditional staining methods based on Coomassie Brilliant Blue dyes can locate protein quantities of approximately 10 ug, and enhanced visualization using silver stains (*27*) has lowered that minimum to approximately 200 ng. For "average" proteins in the 100,000 dalton molecular weight range, these sensitivities therefore correspond to detection of picomoles of sample. In contrast, FT-ICR offers detection of fmol of samples (*17*).

Most critical, however, is the dramatic difference in precision between biochemical molecular weight techniques and FT-ICR. Estimation of molecular weight by SDS-PAGE or gel filtration is indirect, derived from comparison with standards of known mass anlayzed concurrently, and affords resolution within only 500 to 1000 daltons. Analytical ultracentrifugational estimates of molecular weight are obtained directly, generally through low-speed meniscus depletion techniques, but sample preparation and data interpretation can be laborious. Direct determination of protein molecular weights, accomplished by summation of the masses of the constituent amino acids, provides the greatest precision; however, the procedures required for peptide bond hydrolysis also affect other portions of the molecule. Discrimination of glutamic acid and glutamine, for example, must be accomplished separately. None of these shortcomings restricts the applicability of FT-ICR to determination of bimolecular mass. Molecular weight assignments through FT-ICR have already been made for peptides and proteins with molecular weights from 500 to 29,000 (*see Table 1*). The precison of these determinations is particularly vital in the discrimination between similar proteins from different species. The clear distinctions between bovine and porcine insulins (*molecular weights of 5733.5 and 5777.6, respectively*) (*10*) and between horse and sperm whale myoglobin (*molecular weights 17,000 and 17,200, respectively*) (*24,25*), which were readily evident using FT-ICR, would have required complete amino acid sequence data if they were to have been investigated in a biochemical laboratory.

The general use of mass spectrometry in peptide and protein sequencing has been reviewed (*28*). Recent applications of FT-ICR to protein analysis include several examples of protein sequencing. Early experiments that used bombardment desorptions produced ample quantities of molecular ions but often failed to generate a population of fragments sufficient for sequence analysis. The modification of these

TABLE 1.
PROTEINS AND PEPTIDES ANALYZED BY FT-ICR

Protein or peptide	Approximate Molecular Weight	References
leu-enkephalin	555	15
bradykinin	1050	9
gramicidin S	1150	16, 21, 24, 30
angiotensin	1300	8
substance P	1350	29
neurotensin	1670	10
renin substrate tetradeca-peptide (porcine)	1750	29
gramicidin D major component	1880	21, 30
alamethicin	1960	23
atriopeptide III (rat)	2550	29
melittin	2850	10
sex steroid binding protein (rabbit)	3050	29
glucagon	3480	10
insulin (bovine)	5730	10, 25
(porcine)	5780	10
cytochrome c (horse heart)	12,380	10, 25
ribonuclease A (bovine)	13,700	24
lysozyme (chicken egg)	14,300	25
(human milk)	14,700	25
myoglobin (horse)	17,000	24, 25
(sperm whale)	17,200	24, 25
β-lactoglobulin (bovine milk)	18,500	25
trypsin inhibitor (soybean)	21,000	25
carbonic anhydrase (bovine)	29,000	24, 25
lactate dehydrogenase (rabbit skeletal muscle)	35,700	25
ovalbumin (chicken egg)	43,300	12, 25
serum albumin (bovine)	66,000 (monomer)	25
	133,000 (dimer)	25
conalbumin (turkey egg)	77,500	25

methods to include surface-induced dissociation, producing a larger population of daughter ions, allowed the sequencing of a variety of peptides, including rabbit sex steroid-binding protein (*29*). Similarly, fragmentation of laser-desorbed oligopeptide ions by photodissociation facilitated confirmation of the amino acid sequences of gramicidins D and S by FT-ICR (*30,31*). The successes with these two molecules illustrate several advantages of mass spectrometric approaches to sequencing. First, gramicidin D has a formylated N-terminal, which would have prevented traditional end-group analysis, and its C-terminal is atypically esterified with ethanolamine. In addition, gramicidin D is a pentadecapeptide, approximately the upper limit of most sequencing regimes, but its sequence is poorly suited to enzymatic or chemical treatments that would yield fragments of more manageable size. Gramicidin S is a cyclic decapeptide that would require linearization for typical sequence analyses; the FT-ICR sequencing did not require such preparation. In fact, the absolute complementarity of the positive and negative ion spectta of gramicidin S provided strong evidence for its cyclic nature.

In addition to its wide applicability to protein sequencing, FT-ICR remedies two important shortcomings of biochemical sequencing methods. First, sequencing by reductive cycles (*as in the Edman procedure* (*32*), *for example*) necessarily requires a substantial amount of starting material because each successive cycle of amino acid loss has less than a 100% recovery of the remaining peptide. With only a 5% loss per cycle, removal of ten amino acids individually would yield only 60% of the original peptide for continued sequencing. Second, this limitation to 10 or 12 amino acids per sequencing experiment necessitates the cleavage of larger proteins into smaller fragments. The resolution of these fragments, often the most difficult step in the entire project, must be accomplished prior to sequencing of any single fragment. FT-ICR offers a higher upper limit to fragment size and, more importantly, it allows an initial group of fragments desorbed in a staging quadrupole source to be transported and sequenced individually in an adjoining analyzer.

Mass spectrometric analysis has proven useful in structural analyses of oligosaccharides and polysaccharides as well. These molecules can be characterized by combinations of enzymatic and chemical degradations with subsequent identification of the resulting fragments, but resolution of the degradation products is typically very tedious because of the similarities among their many monosaccharide components. Alternatively, many analyses involve chemical derivatizations to provide the volatility needed for gas chromatographic analysis. FT-ICR analysis has been used successfully for characterization of a family of malto-oligosaccharides (*33, 34, 35*) and a group of bacterial capsular polysaccharides (*36,37*), with the only derivatizations required being reduction of the reducing termini of the oligomers. In the latter studies, uncommon monosaccharides (*including* ∝*-L-rhamnose and* β*-D-glucuronic acid*) were readily identified, and some sequence information was obtained.

THEORETICAL BASIS

The advantages of FT-ICR are founded in the utility of passive ExB (*i.e., crossed electric and magnetic fields*) ion traps which analyze sample ions based on differences in their trapped motion. The force acting on an ion in a static magnetic field is described by Equation 1.

$$F = qv_{xy}B \qquad 1$$

F is the Lorentz force generated by the magnetic field (B) acting on an ion of charge q, and v_{xy} is the velocity of the ion perpendicular to the magnetic field lines (*i.e., the component of the velocity vector in the X-Y plane*) . The motion of an ion in the X-Y plane is obtained by equating the Lorentz force to the centrifugal force (*Equation 2*),

$$qv_{xy}B = \frac{mv_{xy}^2}{r} \qquad 2$$

thus,

$$r = \frac{mv_{xy}}{qB} \qquad 3$$

where r is the radius of the orbit and mi is the mass of the ion. Owing to Lorentz force of the magnetic field, a charged particle is constrained to a circular orbit in the X-Y plane. The motion of the ion parallel to the magnetic field lines (*i.e., the component of the velocity vector along the Z-axis*) is superimposed on the orbitally constrained *motion resulting* in a helical trajectory (*38*) (*see Figure 1*). An essential feature of this relationship is that the orbit in the X-Y plane is decoupled from the velocity along the Z-axis.

To constrain ion motion along the Z-axis, an electrostatic potential is imposed perpendicular to the magnetic field. Ions which are placed between charged plates of the same polarity (*P1 and P2*) are repelled by the resultant electric field and therefore are constrained in the region between the plates. In this manner, ion motion in crossed magnetic fields is constrained in the X, Y, and Z directions. Any velocity along the Z-axis will result in the ion oscillating between the trapping plates. Ion motion in a ExB ion trap can therefore be represented as a cylinder, on which the end-to-end oscillation along the Z-axis is superimposed on the cylindrical motion of the orbit in the X-Y plane. Because the frequency of the cyclotron motion, w_c, is inversely proportional to the mass, m (*Equation 4*), the mass-to-charge ratio, m/q, of an ion can be determined by measuring the frequency of the cyclotron motion in a static magnetic field.

$$w_c = \frac{v_{xy}}{r} = \frac{qB}{m} \qquad 4$$

An essential feature of this relationship is that the cyclotron frequency is related to the mass-to-charge ratio and the magnetic field strength and independent of the translational energy. It is also important to note that for a given mass-to-charge ratio and magnetic field strength the radius of the cyclotron orbit is related only to the momentum in the X-Y plane. The FT-ICR signal is obtained by measuring the image current induced in an rf (*radio frequency*) receiver. The detected image current is generated by a coherently orbiting packet of ions. Thus, the key component of the FT-ICR experiment is excitation of an initially random ensemble of ions into a motion that is coherent.

The motivation for high mass applications can be attributed to the method of ion detection (*i.e., the detector does not discriminate against high*

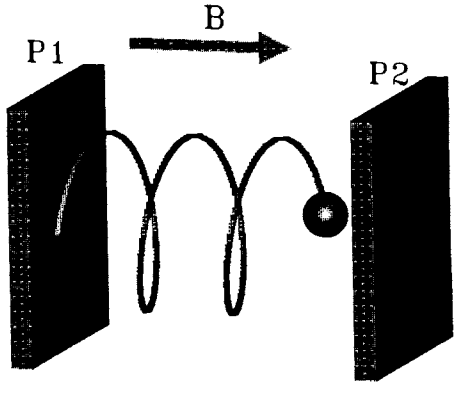

Fig. 1. Cyclotron motion of ions in crossed electric and magnetic fields. Two charged plates (P1 & P2) create an electric field perpendicular to the orbital motion caused by the magnetic field (B). The crossed electric and magnetic fields produce the passive ion trap used in FT-ICR.

mass), the extended mass range of the instrument, and the promise of high resolution at high mass (*2*). The mass range of FT-ICR is directly proportional to the magnetic field strength, B, and inversely dependent on the minimum detectable frequency, f_{min} (*see Equation 5*).

$$\frac{m}{q}(Max.) = 1.54x10^{7}\frac{B}{f_{(min)}} \qquad 5$$

It is the interference by low frequency (*<10kHz*) noise which ultimately limits the upper mass range of the instrument. With suitable precautions to shield the instrument from low frequency noise it is possible to operate in the 3-4 kHz range (*39*), corresponding to an upper mass limit of ca. 90,000 (*B = 7 tesla*). Inherent flexibility and wide mass range combined with the ultra-high mass resolution makes FT-ICR attractive as an analytical method. In contrast to sector instruments, in which mass resolution is dependent on the dimensions of mechanical slits, the FT-ICR mass resolution is dependent upon the magnetic field and the observation time of the time-domain signal (*t*) (*Equation 6*).

$$Resolution = \frac{m}{\Delta m} = 1.8x10^{4}\frac{Bt}{m} \qquad 6$$

The time domain signal is damped by ion-neutral collisions, therefore, the collisional damping rate scales linearly with pressure (*typical values for the collisional damping are* $1x10^{-2}$ $cm^2s^{-1}molecule^{-1}torr^{-1}$). For example, at pressures of $1x10^{-7}$ torr and $1x10^{-8}$ torr, the average time between ion-neutral collisions is aproximately 300 ms and 3 s, respectively. The mass resolutions that can be obtained at these pressures differ by an order of magnitude. The spectrum shown in Figure 2 illustrates the sensitivity and mass resolution which can be obtained by FT-ICR (*10*). The spectrum was acquired from a 100 pmol sample of neurotensin (*m/q* = 1674 amu) dissolved in a glycerol/thioglycerol matrix. In the high resolution narrowband spectrum (*inset of Figure 2*), a mass resolution of ca. 90,000 is obtained with a signal-to-noise ration of greater than 500:1.

LIMITATIONS TO HIGH MASS ANALYSIS

The ability to perform high resolution mass measurements in FT-ICR is dependent upon two principal considerations: first, the duration of the time-domain signal and second, the relationship between orbital frequency and *m/q* ratio. Based on the premise that all ions of a given *m/q* ratio have identical frequencies, the only theoretical mechanism for the de-phasing or loss of synchronous motion of the ion packet (*and therefore loss of resolution*) is related to the collision rate with neutrals. Recent results in high mass analysis suggest that a non theoretical loss of resolution exists for high mass ions injected from external ion sources (*10*). In order to realize the potential of FT-ICR, it is important to investigate other mechanisms for de-phasing of the detected ensemble.

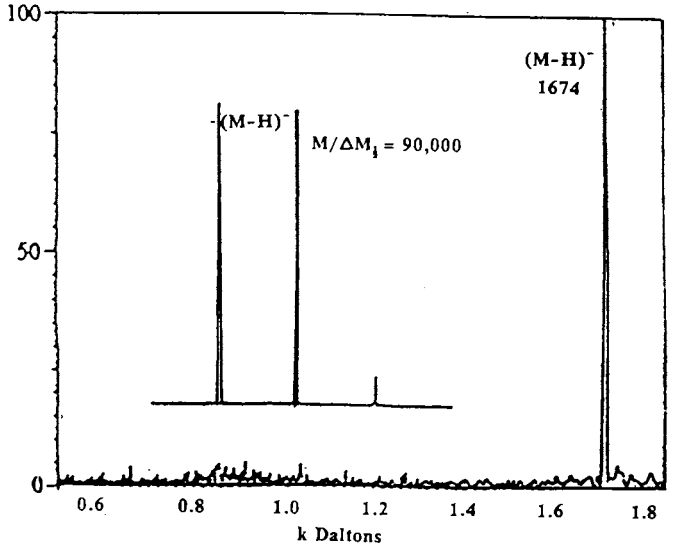

Fig. 2. The mass spectrum of neurotensin (*m/q = 1674 amu*). Mass resolution of ca. 90,000 is obtained with a signal-to-noise ratio of greater than 500:1 from a 100 pmol sample (*Reprinted with permission from reference 10*).

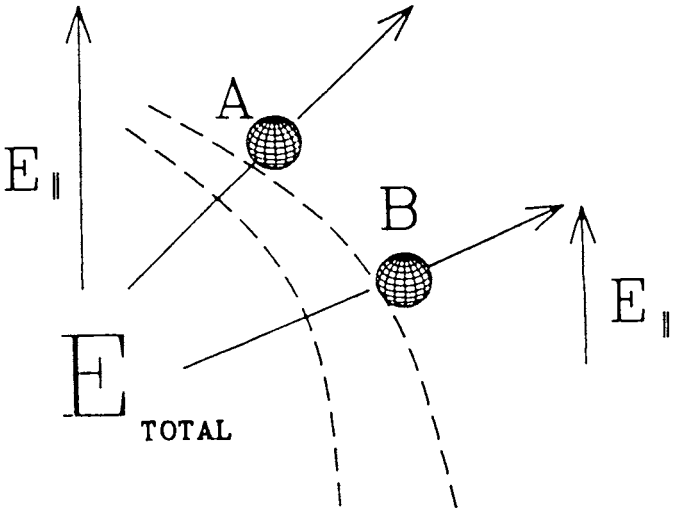

Fig. 3. Electric field generated in a cubic cell. ExB fields produced in an ICR trap have inhomogeneities resulting in electric field forces having components that are both parallel and perpendicular to the magnetic field. Ions having different radii experience different forces depending on location in the cell.

Creation of a "coherent" ion packet prior to ion detection is achieved in FT-ICR through ion acceleration with a linearly polarized alternating (*i.e., radio frequency*) electric field (*40*). The spatial definition of the ion ensemble following excitation has been shown to be strongly dependent upon the initial translational energy of the random ion population (*41*). Although the loss of spatial definition results in a direct loss of signal by increasing the distance between the ions and the receive electrodes (*42,43*), mass resolution is dependent upon the ability to observe the frequency of an ion's orbital motion (*i.e., the duration of the time-domain signal*). The time-domain signal is generated by the induced image current resulting from the phase-synchronous motion of the ion ensemble and not the spatial dimensions.

Detection occurs in the confines of a perpendicular electric field (*ExB*) generated by placing a static voltage on the trap plates of an ion cell having cubic geometry. The electrostatic field is contoured by excite and receive plates in the X-Y plane (*Figure 3*). Owing to the symmetry of a cubic ion cell, high trapping fields placed on the trap plates result in strong radial (*X-Y plane*) potential gradients. Imperfect electric fields having vector components parallel to the magnetic field introduce a new radial force, $E_{||}$, which is perpendicular to the ion's orbit. This new radial force shifts the frequency of the orbital motion resulting in difficulty in mass assignments for measured frequencies (*44,45,46*).

Although the frequency shifts resulting from ion interaction with the DC electric field can be corrected by use of calibration tables (*47*), such calibration tables are useful only if the all ions of a given *m/q* ratio are shifted to the same frequency. If the electric field is homogeneous within the spatial dimensions of the ion packet, the radial force due to the DC electric field is the same for all ions of the packet. However, if

the electric field is inhomogeneous in the dimensions of the ion ensemble, then the ions at different locations will experience different forces. The different radial electric fields result in differences in the orbital frequencies for ions of a single *m/q* value. To address the issues concerning non-collision limited loss of mass resolution for externally produced ions, it is necessary to evaluate the effect of an inhomogeneous DC electric field on an ion ensemble having a broad spatial distribution.

The inhomogeneous electric field causes $E_{||}$ to be positionally dependent and, therefore, the radial component of $E_{||}$ changes as the center of the ion's orbit drifts both axially and radially. The fluctuations in $E_{||}$ result in continuous changes in radial frequency, axial frequency, and magnetron drift by reducing the effective force of the magnetic field.

$$B_{effective} = B - \frac{E_{||}}{v} \qquad 7$$

where $E_{||}$ inhomogeneities are the product of the applied trapping voltage, E_t, and a cell constant, ξ (*48*). Based on these considerations a new equation for resolution based on inhomogeneous fields was derived (*46*).

$$\text{Resolution} \propto \frac{\{B - (m/q)(E_t \xi)\}}{B} t \Big/ m/q \qquad 8$$

From Equation 8, it can be seen that mass resolution is now not only more dependent upon the *m/q* ratio of the detected ions than previously predicted (*Equation 6*), but it can also be shown to be dependent upon the cell geometry and applied trapping voltage.

The impact of a continuously changing $E_{||}$ on orbital frequency is shown in Figure 4. It is important to note that although an ion of *m/q* 100 effectively produces a single frequency (*1.3 ppm deviation as a function of time*), an ion of *m/q* 1000 produces a wide range of frequencies (*1.6×10^4 ppm deviation as a function of time*) due to the changing magnitude of $E_{||}$ (*46*). The poor frequency definition corresponds to a loss of mass resolution for high mass ions. The resultant mass spectrum for these two trajectories can be simulated through Fourier analysis of the Y position as a function of time (*i.e., the time domain spectrum*). Figure 5 is a simulated spectrum for ions of *m/q* 100 and *m/q* 1000 in a cubic trap ($(2.54\ cm)^3$) with 10 volts applied to the trapping plates. Note both the loss of resolution and the shift in the observed mass for the ions of *m/q* 1000 (*46*).

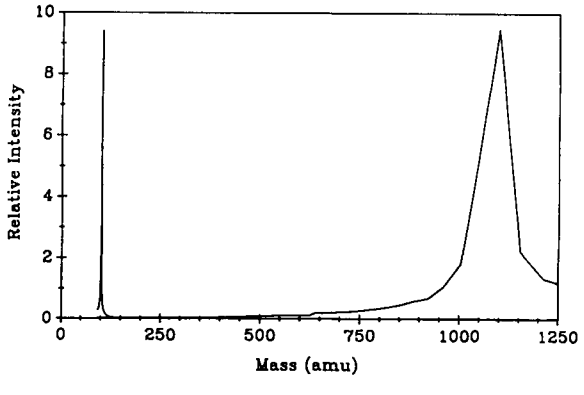

Fig. 4. The impact of $E_{||}$ on orbital frequency. An ion of *m/q* 100 effectively produces a single frequency *(1.3 ppm deviation as a function of time)*, compared to an ion of *m/q* 1000 which produces a wide range of frequencies *(1.6×10^4 ppm deviation as a function of time)* due to the changing magnitude of $E_{||}$. The poor frequency definition corresponds to a loss of mass resolution for high mass ions *(Reprinted from reference 46)*.

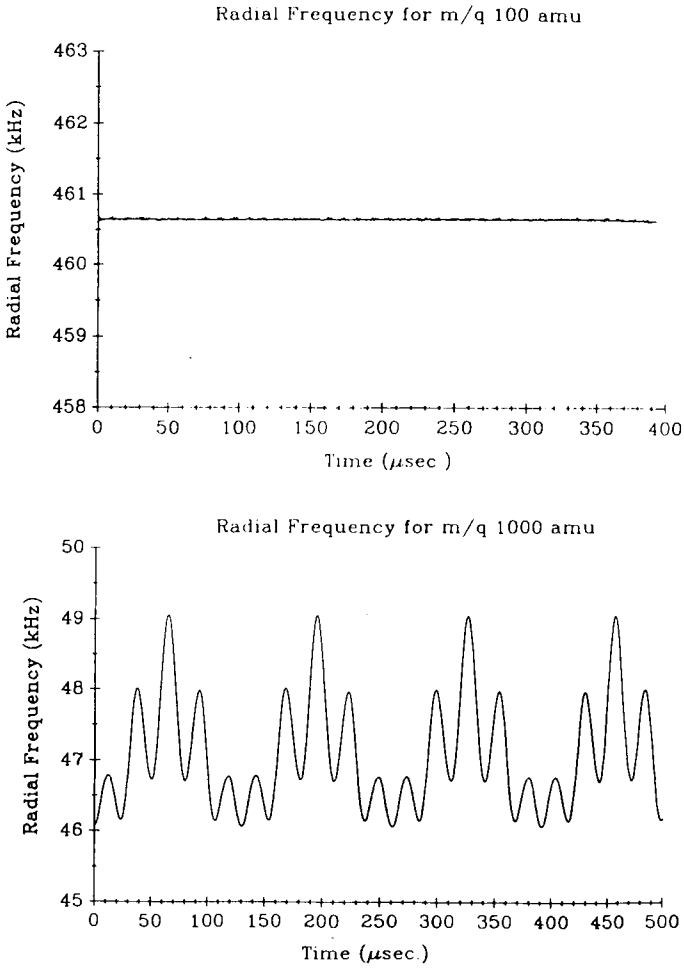

Fig. 5. Comparison of mass resolution in an inhomogeneous ExB ion trap as a function of mass. A simulated spectrum based on the theoretical trajectories of ions of *m/q* 100 and *m/q* 1000 in a cubic trap *($(2.54\ cm)^3$)* with 10 volts applied to the trapping plates illustrates both the loss of resolution and the shift in the observed mass for the ions of *m/q* 1000 *(Reprinted from reference 46)*.

NEW EXCITATION TECHNIQUES

Based on the criteria for detection in ion cyclotron resonance spectroscopy, creation of a "coherent" ion packet prior to detection is vital for high resolution. To be considered coherent, the ions must have similar angles of rotation (*i.e., be at the same point of rotation at the same time*) and have minimal spatial distribution. Because the coherent ion packet is created by the applied rf excitation, the nature of the excitation is critical.

Rf excitation was studied using the numerical simulation program SIMION. Initial studies of excitation determined the effect of resonant rf excitation. In Figure 6, trajectories of four ions of *m/q* 100 (*initially out of phase; angles of 90°, 180°, 270°, and 360°*) are shown during resonant frequency excitation. It is significant to note that all of the ions have reached the same angle of rotation after equal periods of excitation. This trajectory plot illustrates both the creation of phase coherence and the continuous gain of energy due to the rf excitation.

The amount of energy gained during phase synchronization is important due to the finite dimensions of the cell. Figure 7 shows ions of *m/q* 5000 during resonant frequency excitation. The ions are driven to a large radius of rotation during resonant excitation and can exceed

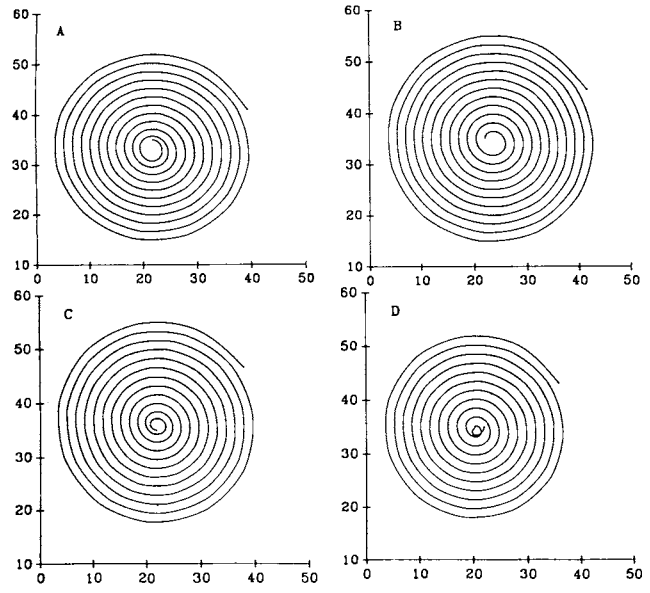

Fig. 6. Ion trajectories during rf excitation. Theoretical trajectories for ions of m/q 100, initially out of phase, during rf excitation. The termination of the four trajectories at the same point in their orbits illustrates that the orbits have become coherent during excitation.

the finite dimensions of the cell prior to coherence. This is due to the direct relationship of *m/q* to radius as expressed in equation 3. Because resonant excitation schemes cannot produce a detectable packet of ions, the ability of swept frequency excitation to create a coherence must be evaluated.

Swept frequency excitation of ions of *m/q* 500 was simulated using SIMION by starting at a frequency of 1590 kHz and sweeping down *(through slower frequencies)* toward the resonant frequency of 92 kHz at a rate of 4 kHz /usec. As seen in Figure 8, swept frequency excitation results in maximal coherence being reached at approximately 790 kHz, long before the applied frequency becomes resonant. Ions that are excited at the resonant frequency have a larger kinetic energy distribution because they are gaining energy during the entire excitation. Conversely, ions excited using swept frequency excitation do not gain energy throughout the entire excitation period due to non resonant frequency interaction. Therefore, the radius does not become as large during swept frequency excitation as it does during resonant frequency excitation because of the lower kinetic energies. Achieving coherence at lower kinetic energies has the advantage of allowing high mass ions to be forced into coherence while still being contained in the ion trap.

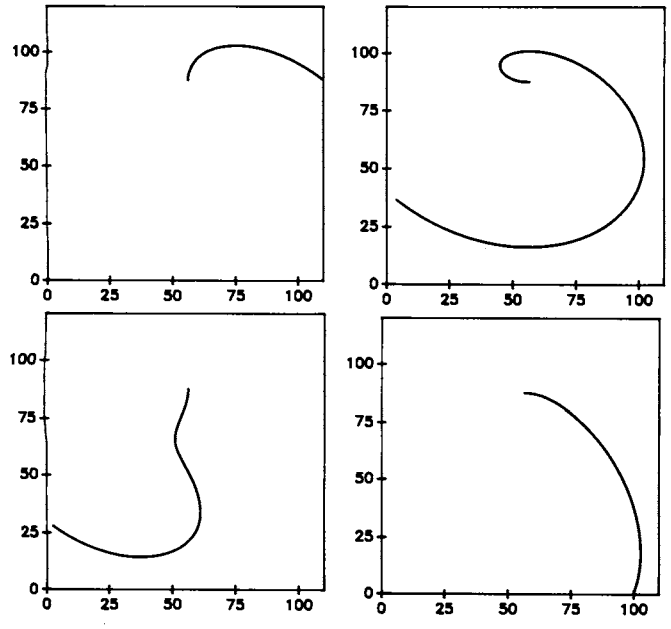

Fig. 7. High mass limitations during rf excitation due to finite cell size. Theoretical ion trajectories for ions of m/q 5000, initially out of phase, during resonant rf excitation. All four ions gain kinetic energy that exceeds the physical boundaries of the cell, resulting in orbit interruption prior to formation of a coherent packet.

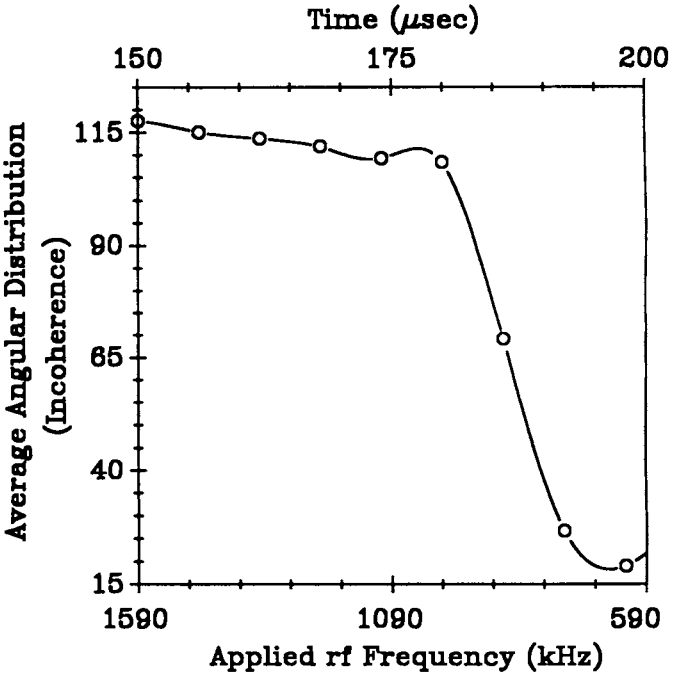

Fig. 8. Induced coherence using non-resonant excitation. A plot of average angular separation *(incoherence)* of ions of m/q 500 during swept frequency indicates that ions reach maximum coherence *(ca. 197 usec)* without resonant frequency excitation.

CONCLUSIONS

With improvements in the isolation and purification of trace components of biological systems, the high sensitivity and resolution of FT-ICR will be important assets to investigations of structure and function. For example, isozymes, or multiple forms of enzymes found in different tissues within the same species, are generally distinguished by their dissimilar kinetic and immunological properties because their structural differences are subtle. The high resolution available through FT-ICR could provide an additional basis for discrimination that would not be dependent on physiologically active forms of the isozymes. As organ specificities and developmental relationships can often be interpreted through isozyme distribution patterns, more sensitive assessment of isozyme occurrences would have a profound impact on investigations in these areas.

Identification of post-translational modifications, some of which occur only singly in a given polypeptide, is difficult with current

biochemical methodologies. For example, phosphorylation of tyrosine, a common modification induced by oncogenic activity in cells, is now detected either by isoelectric focusing techniques or by measurement of the incorporation of ^{32}p-phosphate. FT-ICR would provide resolution superior to the results obtained from the former experiments and would eliminate the need for radioisotopes in the latter experiments. FT-ICR also provides a means to detect rare amino acids like selenocysteine in intact proteins, a task that presently is very challenging.

While structural information is valuable, much of the current interest in proteins is focused on structure-function relationships. Of particular interest is the role played by protein conformational changes during cellular processes, including binding of hormones and substrates and transduction of signals across cell membranes. Attempts to visualize such changes have been made using infrared and NMR spectroscopy, but with limited success. The time-averaging nature of these techniques makes it difficult to identify transient conformations adopted by the target proteins.

The binding of metal ions by proteins has been shown to induce changes in fragmentation susceptibility of the polypeptide chains, generally by introducing new sites of lability near the cations (*49*). It therefore should be possible to distinguish apoproteins from their metalloproteins by FT-ICR. This would be useful in studies of the kinetics of ion associations with proteins. In principle, binding of other ligands by proteins could lead to similar changes in fragmentative behavior; with large enough deformations, the induced lability associated with metal ions would not be necessary. The transient nature of the conformational changes would not present a complication, as the lifetimes of the fragments would be expected to exceed the duration of very rapid phenomena.

Applications of mass spectrometry to bimolecular studies are not limited to analysis of proteins and peptides. Many nucleosides, nucleotides, and nucleic acids have been characterized, including sequencing studies. With the recent introduction of polymerase chain reaction technology (*50*), a powerful method for amplification of DNA sequences, the development of general nucleic acid sequencing by FT-ICR might seem less pressing. However, nonhydrolyzable oligoribonucleotides are finding increasing utility as "antisense RNA" tools to regulate cellular translational efficiencies. These sequences of these small RNAs cannot be verified by traditional biochemical techniques, which depend on selective cleavages of the phosphodiester linkages of the sugar-phosphate backbone, but they could be identified by FT-ICR in a manner similar to that already described for plasma-desorbed oligonucleotide ions (*13,14*). Additionally, many messenger and transfer RNAs, like proteins, contain post-synthetic modifications and unusual components. Methylations of these molecules, and the presence of nonclassical bases like pseudouridine, are characteristic of natively assembled nucleic acids; consequently, they cannot be mimicked and amplified by the polymerase chain reaction. Their nonabundance makes them difficult to discern, but the heightened sensitivity of FT-ICR might afford definitive characterization of these structures.

The versatility of FT-ICR in structural determination has recently been demonstrated in studies of glycoalkaloids, steroid glycosides, and steroids (*51,52*) and in characterization of complex carbohydrates (*36,37,38,39,40*). With the growing interest in oligosaccharides as recognition markers for various normal and abnormal developmental events, and for infectivity of both bacteria and viruses, FT-ICR could provide important information about the molecular structures involved in these phenomena.

ACKNOWLEDGEMENT

We would like to express our gratitude for the funding provided by the Research Corporation (*Cottrell Science Grant*), the Carver Foundation, and the Graduate College at the University of Northern Iowa.

REFERENCES

(1). EADON, G.A. IN *Treatise on Analytical Chemistry,* Part 1, Volume 2, Chapter 1; Ed. Kolthoff-Winefordner; Wiley and Sons, New York, 1989.
(2). WILKINS, C.L.; GROSS, M.L. *Anal. Chem.* 1981, 53, 1661A.
(3). BARBER, M.; BORDOLI, R.S.; SEDGWICK, R.D.; TYLER, A.N. *J. Chem. Soc., Chem. Comm.* 1981, 325.
(4). ABERTH, W.; STRAUB, K.M.; BURLINGAME, A.L. *Anal. Chem.* 1982, 54, 2029.
(5). BENNINGHOVEN, A.; JASPERS, D.; SICHTERMANN, W. *Appl. Phys.* 1976, 11, 35.
(6). CARLSON, E.G.; PAULISSEN, G.T.; HUNT, R.H.; O'NEAL, M.J. *Anal. Chem.* 1960, 32, 1489.
(7). DELL, A.; MORRIS, H. *Biochem. Biophys. Res. Comm.* 1982, 106, 1456.
(8). HUNT, D.F.; SHABANOWITZ, J.; MCIVER, R.T., JR.; HUNTER, R.L.; SYKA, J.E.P. *Anal. Chem.* 1985, 57, 765-768.
(9). HUNT, D.H.; SHABANOWITZ, J.; YATES, J.R., III; MCIVER, R.T., JR.; HUNTER, R.L.; SYKA, J.E.P.; AMY, *J. Anal. Chem.* 1985, 57, 2733-2735.
(10). HUNT, D.H.; SHABANOWITZ, J.; YATES, J.R., III; ZHU, N.-Z.; RUSSELL, D.H.; CASTRO, M.E. *Proc. Natl. Acad. Sci. USA* 1987, 620-623.
(11). SUNDQVIST, B.; ROEPSTORFF, P.; FOHLMAN, J.; HEDIN, A.; HAKANSSON, P.; KAMENSKY, I.; LINDBERG, M.; SALEHPOUR, M.; SAWE, G. *Science* 1984, 226, 696-698.
(12). JONSSON, G.P.; HEDIN, A.B.; HAKANSSON, P.L.; SUNDQVIST, B.U.R.; BENNICH, H.; ROEPSTROFF, P. *Rapid Comm. Mass Spectrom.* 1989, 3, 190-191.
(13). MCNEAL, C.J.; OGILVIE, K.K.; THERIAULT, N.Y.; NEMER, M.J. *J. Am. Chem. Soc.* 1982, 104, 976-980.
(14). MCNEAL, C.J.; OGILVIE, K.K.; THERIAULT, N.Y.; NEMER, M.J. *J. Am. Chem. Soc.* 1982, 104, 981-984.
(15). TABAT, J.C.; RAPIN, J.; PORETTI, M.; GAUMANN, T. *Chimia* 1986, 40, 169-171.
(16). WILLIAMS, E.R.; MCLAFFERTY, F.W. unpublished results, Department of Chemistry, Cornell University, Ithaca, NY.
(17). POSTHUMUS, M.A.; KISTEMAKER, P.G.; MUEZELAAR, H.L.C.; TEN NOEVER DE BRAUW, M.C. *Anal. Chem.* 1978, 50, 985.
(18). KARAS, M.; HILLENKAMP, F. *Anal. Chem.* 1988, 60, 2301-2303.
(19). JONSSON, G.P.; HEDIN, A.B.; HAKANNSON, P.L.; SUNDQVIST, B.U.R.; SAVE, B.G.S.; NIELSEN, P.F.; ROEPSTORFF, P.; JOHANSSON, K.-E.; KAMENSKY, I.; LINDBERG, M.S.L. *Anal. Chem.* 1986, 58, 1084-1087.
(20). MANN, M.; MENG, C.K.; FENN, J.B. *Anal. Chem.* 1989 61, 1702-1708.
(21). WILLIAMS, E.R.; HENRY, K.D.; MCLAFFERTY, F.W. *J. Am. Chem. Soc.,* unpublished results, Department of Chemistry, Cornell University, Ithaca, NY.
(22). DOLE, M.; MACK, L.L.; HINES, R.L.; MOBLEY, R.C.; FERGUSON, L.D.; ALICE, M.G. *J. Chem. Phys.* 1968, 49, 2240-2249.
(23). WILLIAMS, E.R.; FURLONG, J.J.P.; MCLAFFERTY, F.W. unpublished results, Department of Chemistry, Cornell University, Ithaca, NY.
(24). HENRY, K.D.; WILLIAMS, E.R.; WANG, B.H.; MCLAFFERTY, F.W.; SHABANOWITZ, J.; HUNT, D.F. *Proc. Natl. Acad. Sci. USA* 1989, 86, 9075-9078.
(25). LOO, J.A.; UDSETH, H.R.; SMITH, R.D. *Anal. Biochem.* 1989, 179, 404-412.
(26). LAEMMLI, U. *Nature* 1970, 227, 680-685.
(27). MERRIL, C.R.; GOLDMAN, D.; SEDMAN, S.A.; EBERT, M.H. *Science* 1981, 211, 1437-1438.
(28). BIEMANN, K.; MARTIN, S.A. *Mass Spectrometry Reviews* 1987, 6, 1-76.
(29). WILLIAMS, E.R.; HENRY, K.D.; MCLAFFERTY, F.W.; SHABANOWITZ, J.; HUNT, D.F. unpublished results, Department of Chemistry, Cornell University, Ithaca, NY, and Department of Chemistry, University of Virginia, Charlottesville, VA.
(30). CODY, R.B., JR.; AMSTER, I.J.; MCLAFFERTY, F.W. *Proc. Natl. Acad. Sci. USA* 1982, 82, 6367-6370.
(31). YANG, L.-C.; WILKINS, C.L. *Organic Mass Spectrom.* 1989, 24, 409-414.
(32). EDMAN, P. *Acta Chem. Scand.* 1956, 10, 761-768.

(33). COATES, M.L.; WILKINS, C.L. *Biomed. Mass Spectrom.* **1985**, 12, 424-428.
(34). COATES, M.L.; WILKINS, C.L. *Anal. Chem.* **1987**, 59, 197-200.
(35). LAM, Z.; COMISAROW, M.B.; DUTTON, G.G.S. *Anal. Chem.* **1988**, 60, 2304-2306.
(36). LAM, Z.; COMISAROW, M.G.; DUTTON, G.G.S.; WEIL, D.A.; BJARNASON, A. *Rapid Comm. in Mass Spectrom.* **1987**, 1, 83-86.
(37). LAM, Z.; DUTTON, G.G.S.; COMISAROW, M.B.; WEIL, D.A.; BJARNASON, A. *Carbohyd. Res.* **1988**, 180, c1-c7.
(38). PASZKOWSKI, B., IN *Electron Optics*, translation by R.C.G. Leckey, Iliffe Books, LTD., London, **1968**, 1-52.
(39). CASTRO, M.E.; RUSSELL, D.H. *Anal. Chem.* **1984**, 56, 578.
(40). MARSHALL, A.G.; ROE, D.C. *J. Chem. Phys.* **1980**, 73, 1581.
(41). HANSON, C.D.; KERLEY, E.L.; CASTRO, M.E.; RUSSELL, D.H. *Anal. Chem.* **1989**, 61, 2040-2046.
(42). MCIVER, R.T.; HUNTER, R.L.; LEDFORD, E.B.; LOCKE, M.J.; FRANCL, T.J. *Int. J. Mass Spectrom. Ion Proc.* **1981**, 39, 65.
(43). SHOCKELY, W.J. *Appl. Phys.* **1938**, 9, 635.
(44). SHARP, T.E.; EYLER, J.R.; LI, E. *Int. J. Mass Spectrom. Ion Phys.* **1972**, 9, 421.
(45). DUNBAR, R.C. *Int. J. Mass Spectrom. Ion Proc.* **1984**, 91, 2801.
(46). CAPRON, M.; HASKIN, S.; HANSON, C. *J. Iowa Acad. Sci.* In Press
(47). LEDFORD, E.B.; GHADERI, S.; WHITE, R.L.; SPENCER, R.B.; KULKARNI, P.S.; WILKINS, C.L.; GROSS, M.L. *Anal. Chem.* **1980**, 52, 463.
(48). HUNTER, R.L.; SHERMAN, M.G.; MCIVER, R.T. *Int. J. Mass Spectrom. Ion Phys.* **1983**, 50, 259.
(49). HANSON, C.D.; MACMILLAN, J.G. Unpublished work at the University of Northern Iowa, 1991
(50). SAIKI, R.K.; GELFAND, D.H.; STOFFEL, S.; SCHARF, S.J.; HIGUCHI, R.; HORN, G.T.; MULLIS, K.B.; ERLICH, H.A. *Science* **1988**, 239, 487-491.
(51). COATES, M.L.; WILKINS, C.L. *Biomed. and Environ. Mass Spectrom.* **1986**, 13, 199-204.
(52). FUNG, E.T.; WILKINS, C.L. *Biomed. and Environ. Mass Spectrom.* **1988**, 15, 609-613.